MODELLING THE DEVELOPMENT OF NATURAL HYDROTHERMAL ERUPTIONS

Brett J. Bercich and Robert McKibbin[1]
Department of Engineering Science, School of Engineering
'University of Auckland, Private Bag, Auckland

ABSTRACT - This paper continues and consolidates earlier work (McKibbin, **1989, 1990)** on preliminary mathematical modelling of hydrothermal eruptions which concentrated *on* modelling the underground process. The fundamental equations of motion and thermodynamics are solved in order to examine the properties of an expanding two-phase fluid rising vertically through porous rock and ejecting rock particles at the surface.

The first models relied on a simple homogeneous Darcy's Law to calculate the pressure gradients underground. However, results showed that modifications are required. Here the effects of adding a non-linear (Forchheimer) term to the momentum equation are investigated. Numerical experiments reveal this term to be important when rock permeabilities are relatively large.

The motion of the two boundaries, the "flashing front" and "erosion surface", are examined here. The assumption (McKibbin, 1989) that the two fronts advance downward at the same rate is modified here by using some results given in McKibbin **(1990)** which allow a separate estimate to be made of the "flashing front" speed. The distance between the two boundaries, which gives the thickness of the flashing zone, is found to increase with time; the "flashing front" moves faster than the eroding surface, whilst both are decelerating. Further work involving the effects of cohesive rock stress is dealt with briefly.

1. INTRODUCTION

Hydrothermal eruptions are rare phenomenon that are known to occur in many of the geothermal fields around the world. Besides the rare reported physical witnessing of an eruption taking place, most evidence is based upon breccia deposits on the surface or the discovery of subsurface formations which record the history of many previous eruptions.

Hydrothermal eruptions are categorised as being natural or induced. Natural eruptions include prehistoric and unexploited-field eruptions. Prehistoric eruptions have occurred in Whakarewarewa, Orakeikorako, Rotokawa and other regions of the Taupo Volcanic Zone. Waimangu has more recently been the area of interest for natural eruptions, the latest occurrence being in 1973. Induced eruptions occur as a result of exploitation of geothermal fields. These have taken place in the Tauhara Field and the "Craters of the Moon" area of the Wairakei Geothermal Field.

Hydrothermal eruptions are violent in nature and can last from a matter of minutes to several hours. A hydrothermal eruption is distinct from a geyser in that the former is non-cyclic in occurrence, takes place without warning, and the ejected material is not wet steam but a slushy mixture of two-phase water and rock particles of all sizes. Most of this material is directed vertically upwards from vents that *can* be from 5 m to 500 m in diameter. However, differences in horizontal and vertical in-situ rock stresses can lead to material being directed laterally fkom the vent.

The subject of this work will be restricted to the modelling of natural hydrothermal eruptions with emphasis on the underground mechanism. Appropriate forms for models of existing ambient underground pressure gradients and the rôles played by the form-drag on the rock particles and cohesive stresses are dealt with. The relative motions of the eroding surface and flashing front are investigated.

2. THE MECHANISM

2.1 Causes

The main driving force of natural hydrothermal eruptions is hypothesised as being due to an increased pressure gradient immediately below the surface of the ground arising from the fluid near the surface being suddenly exposed to atmospheric conditions. Possible mechanisms whereby this occurs are discussed by McKibbin **(1989,1990).**

2.2 Consideration of stresses acting

In order for a particle of rock below the surface to be moved, the equilibrium of forces must be upset. During a hydrothermal eruption the force equilibrium is disturbed such that the rock is thrown vertically upward.

In *summary,* it is supposed that hot fluid, initially at rest in the rock matrix, begins to escape to the atmospheric conditions at the surface, flashing and increasing in specific volume as the pressure decreases. The increasing velocity of the fluid as it nears the surface provides lift to the rock particles. A hydrothermal eruption *can* take place when the velocity is great enough to eject the particles, i.e., the net lift is large enough to overcome the weight and cohesive stresses of the rock. The concept is based on mining by steam lifting, rather than by sudden explosions such as those caused by phreatomagmatic phenomena.

3. THE MATHEMATICAL MODEL

Progress made so far pertains to modelling of the process underground. Concern has been limited to the motion of the flashing fluid and the progression of the eroding surface and the flashing front, both of which may be considered to be moving boundaries. A number of simplifying assumptions were made in order to make the earlier modelling feasible; as mentioned above, some of these are modified in this work. The motion above ground is more complicated and is not dealt with here.

3.1 Assumptions

The main assumptions are:

1. The principles of conservation of mass, momentum and *energy* hold.

2. The fluid below the flashing zone is motionless.

3. The flowing fluid is a homogeneous mixture of liquid and steam. Owing to the fact that boiling occurs very quickly, time is not available for the two separate phases to be established in their passage to the surface.

4. The moving fluid is at saturated (boiling) conditions.

5. The process is quasi-steady, i.e., the eruption has already been initiated and is currently in progress, and is modelled as being nearly steady.

6. The fluid lifts the rock particles at the surface, where conditions are atmospheric (T = 100 °C).

7. Thermal conduction is ignored, i.e., there is no heat transfer between the fluid and rock in the flashing zone. The process is modelled as being adiabatic.

3.2 Preliminary theory

There are two moving boundaries to the flashing zone where underground fluid movement is taking place. The lower boundary, termed the "flashing fiont", propagates downward into the stationary fluid in the rock matrix at *speed* V. The boundary formed by the eroding ground surface above also propagates downward; its speed is V_{er}. The early models assumed that $V_{er} = V$ but this is not justifiable, nor was it necessary for the calculations previously carried out.

The flashing front moves at speed V into a fluid-filled medium of porosity ϕ where the fluid has liquid saturation $S_{\ell d}$, density ρ_{fd}, and specific enthalpy h_{fd} [parameters concerned with conditions at depth have a 'd' subscript whilst those associated with conditions at the top (eroding) surface, where T = 100 °C and p = 1 bar, have a 't' subscript]. The average fluid particle velocity is $\mathbf{V}_f$. Subcripts f, r, ℓ and v denote fluid, rock, liquid water and vapour respectively.

The technique is to set up, and refer all moving quantities relative to, a frame of reference which moves downward at the same speed V as the flashing fkont (see Figure 1). Because the motion is assumed to be quasi-steady, the frame of reference can be treated as inertial for the short periods of time considered. Within this frame, the flow is assumed steady.

3.3 Equations for the underground flow

Conservation of mass

Figure 1(a) shows the flashing front moving into a motionless fluid in the pores of the medium. The constant mass flowrate per unit area through this region and the flashing zone is, relative to the moving frame of axes [Figure 1(b)],

$$m_f = \phi\rho_f(V + V_f)$$

but at the "flashing fiont", $V_f = 0$, and hence

$$m_f = \phi\rho_f(V + V_f) = \phi\rho_{fd}V \qquad (1)$$

The rock has zero absolute velocity. Relative to the moving frame, the rock mass flowrate m_r is constant and is given by

$$m_r = (1 - \phi)\rho_r V \qquad (2)$$

The fluid mixture densities ρ_f, ρ_{fd} are

$$\rho_f = S_\ell\rho_\ell + (1 - S_\ell)\rho_v \qquad (3)$$

$$\rho_{fd} = S_{\ell d}\rho_{\ell d} + (1 - S_{\ell d})\rho_{vd}$$

where ρ is the density and S_ℓ is the liquid saturation (volume fraction of liquid in the two-phase fluid).

Conservation of momentum

The fluid volume flowrate per unit area w_f relative to the moving frame of axes is given by the simple Darcy's Law:

$$w_f = \frac{k}{\mu_f}\left(-\frac{dp}{dz} - \rho_f g\right) + \phi V \qquad (4)$$

where the term ϕV is associated with the moving reference frame. For the boiling mixture, the dynamic viscosity is taken to be

$$\mu_f = \mu_\ell^{S_\ell}\mu_v^{(1 - S_\ell)}$$

With the assumption that the boiling fluid is moving as a homogeneous two-phase mixture, the separate liquid and vapour mass flowrates per unit area are

$$m_\ell = S_\ell\rho_\ell w_f \quad \text{and} \quad m_v = (1 - S_\ell)\rho_v w_f$$

and the total mass flow per unit area is

$$m_f = m_\ell + m_v = \rho_f w_f$$

Substitution into Equation (1), rearrangement and use of Equation (4) gives

$$V_f = \left(\frac{\rho_{fd}}{\rho_f} - 1\right)V = \frac{k}{\phi\mu_f}\left(-\frac{dp}{dz} - \rho_f g\right) \qquad (5)$$

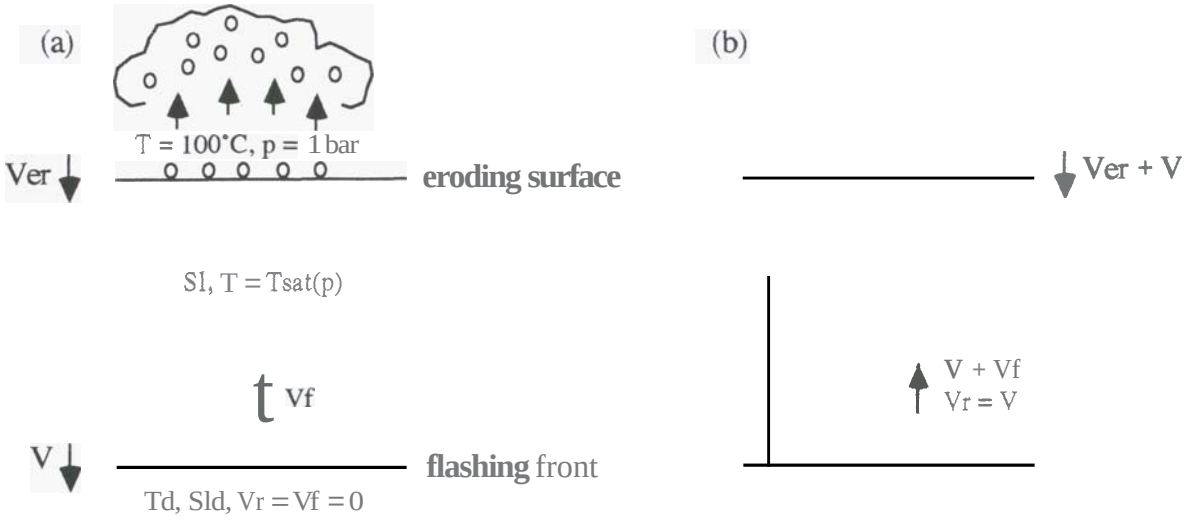

Figure 1 Schematic of flows: (a) relative to fixed axes; (b) relative to frame of reference moving downwards with flashing front.

From Equation (1) it can also be deduced, by applying the surface boundary conditions, that

$$V = \frac{V_{ft}}{\frac{\rho_{fd}}{\rho_{ft}} - 1} - \frac{V_{ft}}{\frac{v_{ft}}{v_{fd}} - 1} \qquad (6)$$

where v is the specific volume. This equation relates the flashing fiont speed to the speed and density of the fluid as it reaches the surface. The overall volume expansion factor for the flashing fluid as it rises from the bottom to the surface is given by

$$v_{rat} = \frac{v_{ft}}{v_{fd}} = \frac{\rho_{fd}}{\rho_{ft}} \qquad (7)$$

Conservation of energy

The vertical energy flowrate per unit area is

$$q_e = m_\ell h_\ell + m_v h_v = m_f h_f$$

where

$$h_f = \frac{\rho_v h_v + S_\ell (\rho_\ell h_\ell - \rho_v h_v)}{S_\ell \rho_\ell + (1 - S_\ell)\rho_v} \qquad (8)$$

is the flowing enthalpy of the fluid. Boundary conditions at the flashing front give

$$q_e = m_f h_{fd}$$

Because q_e is conserved, $h_f = h_{fd}$ and the fluid flow is isenthalpic. Rearrangement of Equation (8) gives the liquid saturation in terms of the flowing enthalpy:

$$S_\ell = \frac{\rho_v (h_v - h_f)}{(\rho_\ell - \rho_v) h_f - (\rho_\ell h_\ell - \rho_v h_v)} \qquad (9)$$

and the enthalpy at the flashing fkont is given by

$$h_{fd} = \frac{\rho_{vd} h_{vd} + S_{\ell d} (\rho_{\ell d} h_{\ell d} - \rho_{vd} h_{vd})}{\rho_{fd}} \qquad (10)$$

Equation (5) can be rearranged to give an expression for the pressure gradient :

$$\frac{dp}{dz} = -\rho_f g - \frac{\mu_f \phi V}{k}\left(\frac{\rho_{fd}}{\rho_f} - 1\right) \qquad (11)$$

3.4 Equation of state

The fluid is assumed to be at saturated (boiling) conditions and the equation of state is

$$P = p_{sat}(T) \qquad (12)$$

with

$$\left(\frac{dT}{dp}\right)_{sat} = \frac{(v_v - v_\ell)(T + 273.15)}{h_v - h_\ell} \qquad (13)$$

3.5 Lift condition

The condition required for a rock particle to lift off at the surface is now considered. The hydrodynamic lift at the surface is given in terms of the relative speed of the fluid with respect to the rock by

$$L_t = \frac{3}{4} C_{ds} \frac{1-\phi}{\phi \phi_s d_p} \rho_{ft} |V_{ft} - V_r| (V_{ft} - V_r) \qquad (14)$$

where $\phi_s = 1.0$ for spheres and $C_{ds} = 0.38$ for $Re \geq 1500$ (see McKibbin, 1989). Assuming no in-situ cohesive stresses, the criterion that the dynamic lift exceed the effective weight of the rock is

$$L_t \geq \phi (1 - \phi) (\rho_r - \rho_{ft}) g \qquad (15)$$

The most important parameter of interest is the fluid particle velocity at the surface. This is found by considering the lift condition Equations (14) and (15).

With the knowledge that just below the eroding surface, $V_r = 0$, and V_f is to be determined just at the point where the net lift is zero, substitution of Equation (14) into Equation (15) with equality, and rearrangement gives

$$V_{ft} = \sqrt{\frac{\phi^2 \phi_s d_p}{\frac{3}{4} C_{ds}} \left(\frac{\rho_r}{\rho_{ft}} - 1\right) g}$$

Given the temperature of the fluid at the flashing fiont, the bottom boundary conditions are determined using correlations to find the pressure (at saturated conditions), densities, and enthalpies. The surface is assumed to be at atmospheric pressure. Equation (7) provides the volume expansion factor v_{rat} and the flashing fiont speed V may be found from Equation (6).

The Reynolds number for the flow at the surface is given by

$$Re_t = \frac{\rho_{ft} d_p V_{ft}}{\mu_{ft}}$$

Results (McKibbin, 1990) show that, for a reservoir temperature above 100 °C, the maximum fluid expansion occurs when $S_{\ell d} = 1.0$; the flashing front speed also appears smallest for $S_{\ell d} = 1.0$. Reynolds numbers for any liquid saturation are of the order of at least 100,000. One of the major benefits of this procedure was provision of an estimate of the thickness of the flashing zone. Some interesting qualitative information resulted for particular experimental cases. The reader is referred to McKibbin (1990) for these results.

Modification for cohesive stresses

The properties of the fluid as it makes its way to the surface are traced by integration of Equation (11). At each step of the integration, the lift condition (15) is tested. If a non-zero in-situ cohesive stress is allowed for, the lift criterion becomes

$$L_t - \phi(1 - 4)(\rho_r - \rho_{ft}) g \geq \text{cohesion} \qquad (15a)$$

When this equation is satisfied, lift-off of the first rock particle is said to have occurred.

4. A MODIFICATION TO DARCY'S LAW

4.1 Consideration of form-drag

The model used in experiments so far described the fluid as a homogeneous mixture of liquid and steam with an associated uni-directional pressure gradient governed by the simple single-phase Darcy's Law, given by Equation (11).

The results obtained are valid for laminar flow of the fluid, with Re < 1.0. However, calculations suggest Reynolds number values of approximately 100,000 are more appropriate for the flow at the outlet of the eruption (see McKibbin, 1990). A modification to the simple Darcy relation is needed. This involves introducing a quadratic term in the force balance to account for the predominating form-drag that the fluid particles encounter at the high velocities experienced in the eruption. Surface drag no longer dominates but fluid particle encounters with solid obstacles lead to form-drag increasing in magnitude. The modification is made thus (Nield, 1990):

$$\frac{dp}{dz} = -\rho_f g - \frac{\mu_f}{k} q_f - \frac{C\rho_f}{\sqrt{k}} q_f^2 \qquad (16)$$

where $q_f = \phi V_f$ is the Darcy velocity, or specific volume flowrate of the fluid, relative to the rock matrix. The last, quadratic, term is known as the Forchheimer term. The parameter C is a dimensionless form-drag constant, which depends on the geometric properties of the rock particles in the porous medium.

Now consider the Darcy velocity, $q_f = w_f - \phi V$. From Equation (5),

$$q_f = \phi V_f = \phi\left(\frac{\rho_{fd}}{\rho_f} - 1\right) V$$

Substitution into Equation (16) gives

$$\frac{dp}{dz} = -\rho_f g - \frac{\phi V}{k}\left(\frac{\rho_{fd}}{\rho_f} - 1\right)\left(C\phi V\sqrt{k}(\rho_{fd} - \rho_f) + \mu_f\right) \qquad (17)$$

Numerical experiments were performed using representative parameters that were thought to be typical of the physical problem in order to study the effect of various values of the form-drag coefficient C. The parameters for two cases studied are listed in Table 1.

parameter	Case 1	Case 2
T_d	150 °C	150 °C
$S_{\ell d}$	1.0	1.0
ϕ	0.2	0.2
d_p	0.1 m	0.1 m
k	1.0×10^{-12} m^2	10.0×10^{-12} m^2
4	1500 kg/m^3	1500 kg/m^3
V	0.1 m/s	0.2 m/s

Table 1: Parameter list for Cases 1 and 2.

The form-drag coefficient C was varied from 0 to 5.0 and particular attention was paid to the value C = 0.55, which was originally proposed as an acceptable universal constant (see reference to the paper by Ward in Nield, 1990). An arbitrary cohesive stress of 5000 Pa/m was chosen.

Properties of interest were the pressure p, temperature T, liquid saturation S_ℓ, fluid velocity V_f and the hydrodynamic lift. Their values were plotted at integration steps above the flashing front.

Figures 2 and 3 show how these properties vary for cases 1 and 2 respectively when C is chosen to be 0, 1.0, 0.55, and 5.0. In particular, the pressure profiles give an idea of the importance of the non-linearity in the modified Darcy's Law.

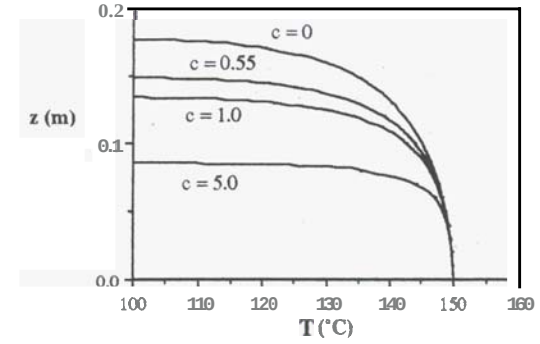

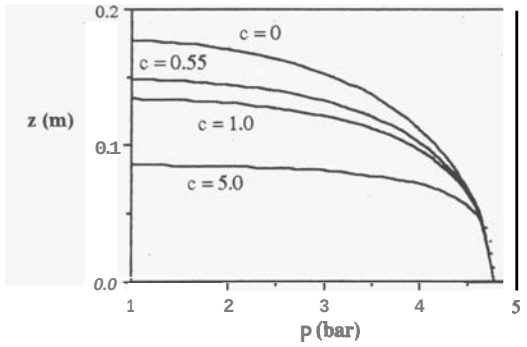

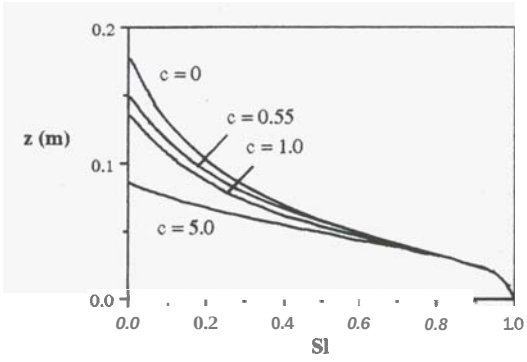

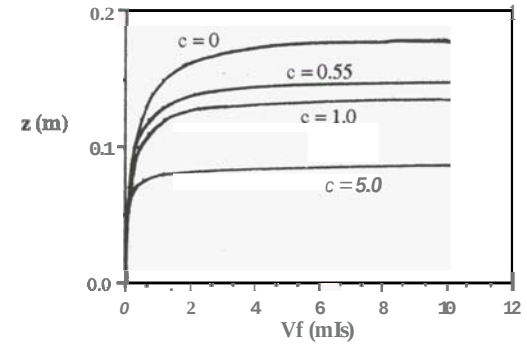

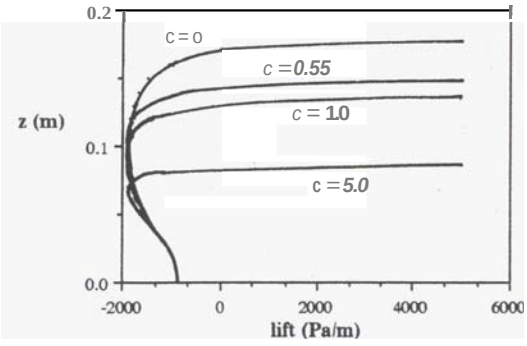

Figure 2 Fluid and physical property parameters for flow. Case 1: k = 1 Darcy, V = 0.1 m/s.

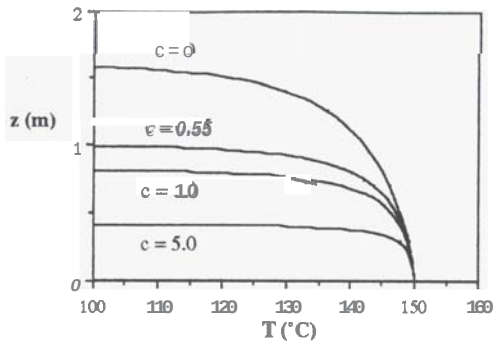

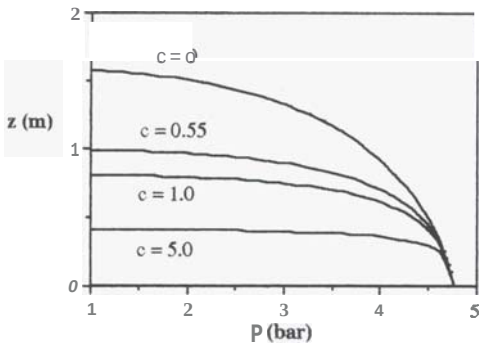

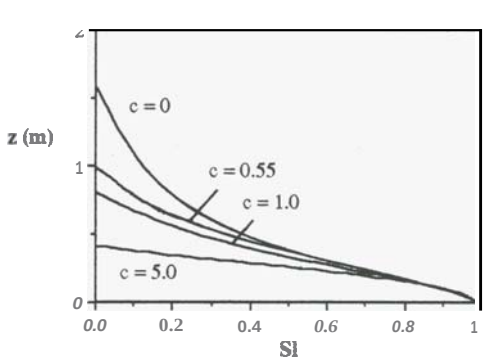

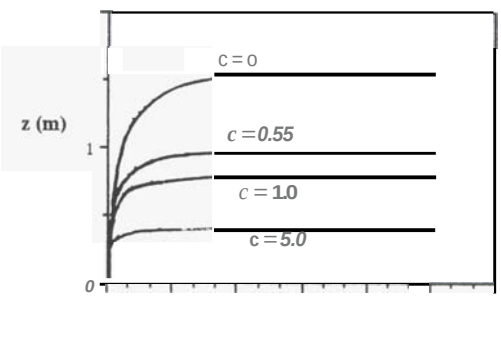

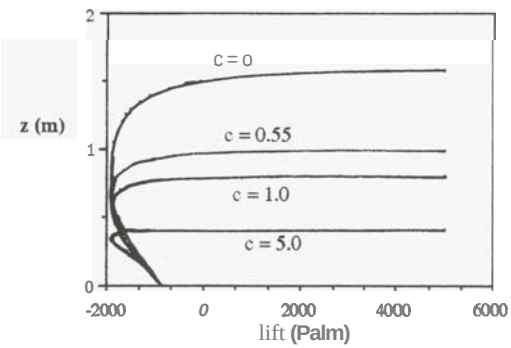

Figure 3 Fluid and physical property parameters for flow. Case 2: k = 10 Darcy, V = 0.2 m/s.

Previous work suggests that the thickness is proportional to the permeability but how does the complication of form-drag affect the thickness? Results are plotted for the two cases in Figure 4.

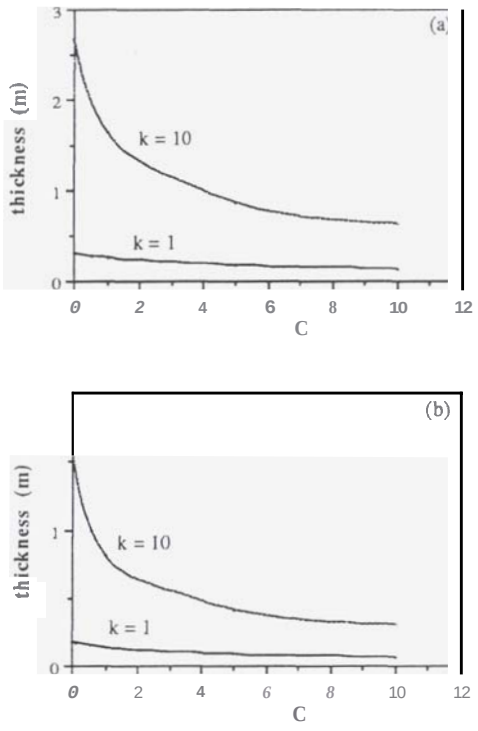

Figure 4 Variation of flashing zone thickness with form-drag coefficient C for k = 1, 10 Darcy. (a) cohesion = 0; (b) cohesion = 5000 Pa/m.

Fluid properties

Temperature, presswe, liquid saturation, fluid velocity and lift follow the same general trends established in the previous investigations where form-drag was ignored. Those results correspond to the curves for C = 0. As expected, the liquid saturation decreases markedly with height. This is a feature of the expansion of the increasingly vapour-dominated flow as it approaches the surface. The more mobile vapour-dominated fluid increases in velocity, a consequence being high Reynolds numbers, and the lift increases sharply immediately below the surface. The 'kink' in the lift profile is caused by the decreased buoyancy offered to the rock particles as the fluid begins to flash and decrease in density while the fluid velocities are small (McKibbin, 1990).

As the form-drag coefficient is increased the thickness of the flashing zone decreases, as one might intuitively expect. The effect is to 'squash' the profiles leading to changes in T, p, S_ℓ, V_f and lift occuring over shorter distances. The profiles become exaggerated for the high form-drag coefficient value of 5.0.

Pressure profiles

The pressure profiles in Figures 2 and 3 indicate the relevance of the Forchheimer term depending on the choice of the permeability k. In either of the cases k = 1.0 Darcy or 10.0 Darcy, the pressure decreases quickly in the region immediately below the eroding surface. This is particularly noticeable for large values of C. These large pressure gradients near the surface reinforce the evidence of increasing hydrodynamic lift near the surface. These pressure gradients also suggest that the quadratic (Forchheimer) term is of more importance when k is large.

Thickness variation with form-drag

The results illustrated in Figure 2 indicate that for k = 1.0 Darcy the simple Darcy's Law (11) is a reasonable approximation to use. The flashing zone thickness over the range of values of C varies fiom 18 cm to 9 cm. However, the quadratic term takes on greater significance for the higher permeability of k = 10.0 Darcy (see Figure 3). In this case thickness variations fiom 1.6 m to 0.4 m are seen. The modified Darcy's Law (17) appears to be the more appropriate form to use.

The relationship between flashing-zone thickness and C is non-linear (Figure 4). It appears unnecessary to consider values of C above 5.0 because form-drag of such large magnitude would not be realistic. The curves appear to asymptote to zero thickness for high values of C.

5. THE MOTION OF THE UPPER BOUNDARY

In earlier work, the speed of the eroding surface was assumed to be the same as that of the flashing front (McKibbin, 1989). Several questions arise:

- How realistic is this assumption ?
- How do the two boundaries move relative to one another?
- Is it possible to trace the motion forward through time and find any reason why it might eventually stop? Can one then go "back in time" and glean some information about the phenomenon's initiation ?

5.1 Theory on the eroding surface

If one considers the process at some time t, the flashing front is moving downwards at a speed V which is solely dependent on the temperature in the reservoir, given other fixed parameters such as ϕ, $S_{\ell d}$, and k. The temperature at the flashing front at a given time during the process is dictated by the ambient temperature gradient underground. For present purposes, it will be assumed that this gradient is constant. If the flashing fiont is at temperature T at time t then its speed may be calculated using Equation (6).

The distance between the two boundaries for a given flashing front temperature and velocity is found by numerical integration of Equation (17). At time t let the thickness be z_1. The downward speed of the eroding surface V_{er} is given approximately by

$$V_{er} = \frac{\text{change in displacement}}{\text{change in time}} = \frac{\Delta z_{er}}{\text{At}}$$

Figure 5 illustrates what is happening over time. At time t + At the flashing front is a distance $V\Delta t$ below the level at t, and because of the temperature gradient, it is at a new temperature T + AT. This new temperature can now be used to determine the new thickness z_2, again by integration. Hence an estimate for V_{er} is

$$V_{er} = \frac{\Delta z_{er}}{\Delta t} = \frac{z_1 + V\Delta t - z_2}{\Delta t} \quad \text{or}$$

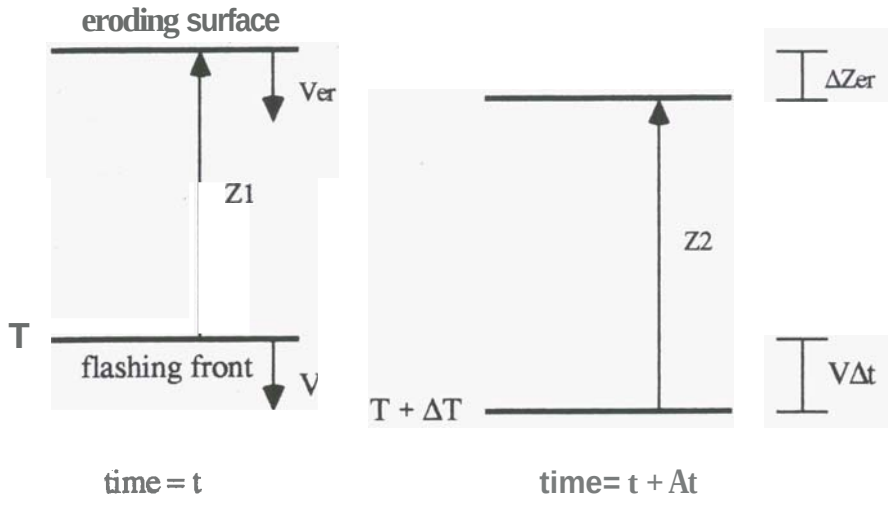

Figure 5 Schematic for calculation of speeds of the flashing front and the erosion surface over time-step At.

$$V_{er} = V + \frac{z_1 - z_2}{\Delta t} \quad (18)$$

The flashing front speed, temperature gradient and time interval are related in the following fashion:

$$V\Delta t \times \frac{dT}{dz} = AT \quad (19)$$

Rearranging,

$$At = \frac{AT}{V \frac{dT}{dz}} \quad (19a)$$

Hence the time interval varies with V if AT, the temperature step size, and dT/dz, the temperature gradient, are chosen appropriately. The means by which one can plot the variation of the two boundary speeds is now available. An initial flashing front temperature T_{d1} is chosen, as are the (constant) temperature gradient and the desired temperature step size. The first flashing front speed V_1 is then determined from Equation (6), then the corresponding thickness z_1 is found fiom integration. Now time advances to the point where the flashing front temperature is T_{d1} + AT = T_{d2}. Again, V_2 and z_2 are found in similar fashion to those at time t. An approximation to the erosion velocity at time t can now be calculated from Equation (18).

5.2 Experimentation

Numerical experiments were performed to see how the front velocities and displacements were affected by "mixing and matching" different temperature intervals and temperature gradients. The following parameters remained constant throughout :

$\phi = 0.2$, k = 10.0 Darcy, $d_p = 0.1$ m, C = 0, $S_{\ell d} = 1.0$

These first experiments were initiated at a flashing front temperature of 130 °C and stopped at 160 'C. Various temperature intervals of 2.5, 5, and 10 K and temperature gradients of – 2, –5, and –10 K/m were used.

The ability to "go back in time" exists by simply starting the flashing front with a lower initial reservoir temperature. An initial temperature of 110 °C was used but no additional information could be gleaned fiom such results.

Example results for velocities V and displacement Y are plotted in Figure 6, for AT = 5 K and dT/dz = –2 K/m. The plots show that, as time proceeds, the flashing zone thickness increases as the flashing front propagates. The eroding surface travels slower than the flashing front. Both boundaries appear to be slowing down with the eroding surface decelerating faster than the flashing fiont.

5.3 Accurate temperature gradients

Ambient reservoir temperature gradients appropriate to the condition of liquid on the point of boiling were calculated. It was thought that a constant gradient, for example, might not accurately represent the "boiling-point-with-depth curve" often thought to exist beneath the ground surface. A program was written to generate accurate estimates of temperature gradients at specific temperatures. This relies on the equation of state :

$$T = T_{sat}(p) \quad (20)$$

The pressure gradient is given by

$$\frac{dp}{dz} = -\rho_\ell(T_{sat})g \quad (21)$$

The temperature gradient at saturated (boiling) conditions is

$$\frac{dT}{dz} = \left(\frac{dT}{dp}\right)_{sat} \frac{dp}{dz} = \left(\frac{dT}{dp}\right)_{sat} (-\rho_\ell(T_{sat})g) \quad (22)$$

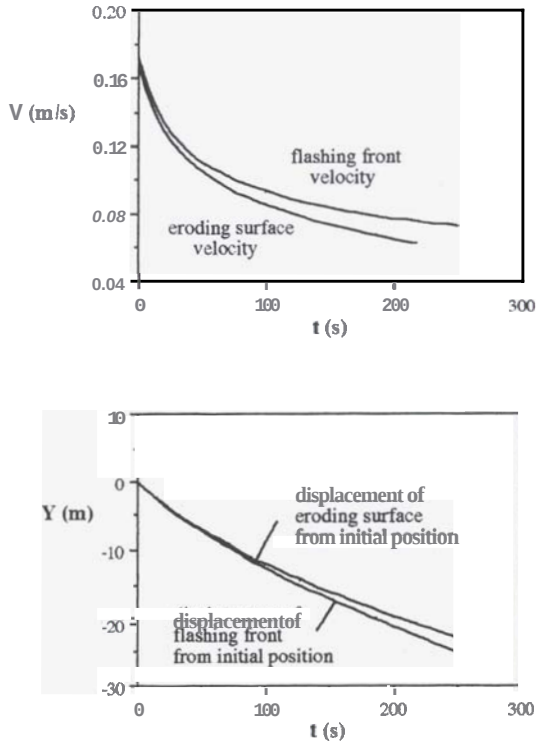

Figure 6 Speed and displacement of the flashing front and the erosion surface as functions of time for the *case* AT = 5 K, dT/dz = –2 K/m.

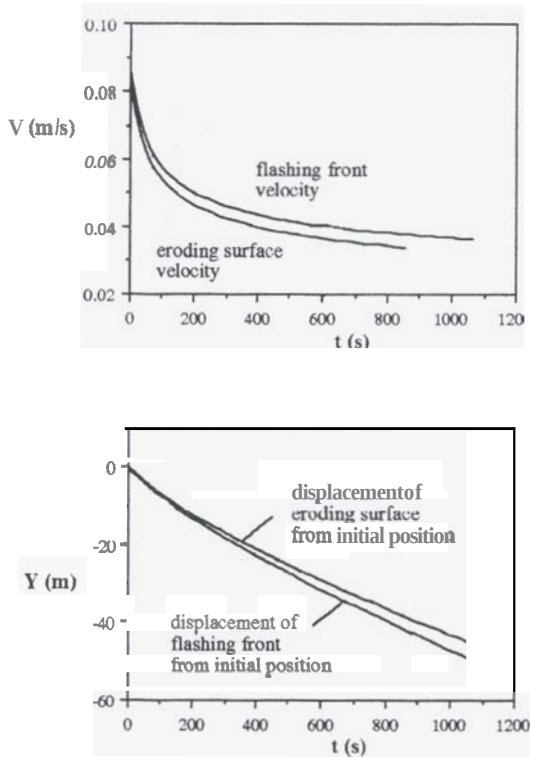

Figure 7 Boundary speeds and displacements for the *case* k = 10 Darcy, cohesion = 0 Pa/m over the temperature range T = 110 to 160 'C.

5.4 The effects of cohesion

Flashing zone thicknesses for flashing front temperatures in the range 110 'C to 160 'C were calculated for both zero cohesive stresses and a cohesion of 5000 Pa/m, combined with "boiling-point-with-depth" temperatures at selected points in this temperature range. Results are plotted in Figures 7 and 8. In Figure 7 the following parameters apply:

k = 10.0 Darcy, ϕ = 0.2, $S_{\ell d}$ = 1.0, d_p = 0.1 m
cohesion = 0 Pa/m , AT = 5 K

In Figure 8 the parameters were the same as the above *case* but cohesion = 5000 Pa/m.

Two interesting features of these results become evident. When there is non-zero cohesion, both the flashing front and the eroding surface slow down at a faster rate than for the zero-cohesion case. A counter-intuitive result also appears: the thickness of the flashing zone at a point in time for cohesion = 5000 Pa/m is smaller than that corresponding to no cohesion at the same moment in time. Why should this occur?

Experimentation revealed that large values of the flashing front velocity result in thin flashing zone thicknesses. Now, from this model, if cohesion increases then the fluid velocity at the surface increases which results in a corresponding increase in the flashing front velocity. This increase in V means that the thickness will decrease. Hence, increasing the cohesive stresses results in a thickness reduction. The model is therefore consistent.

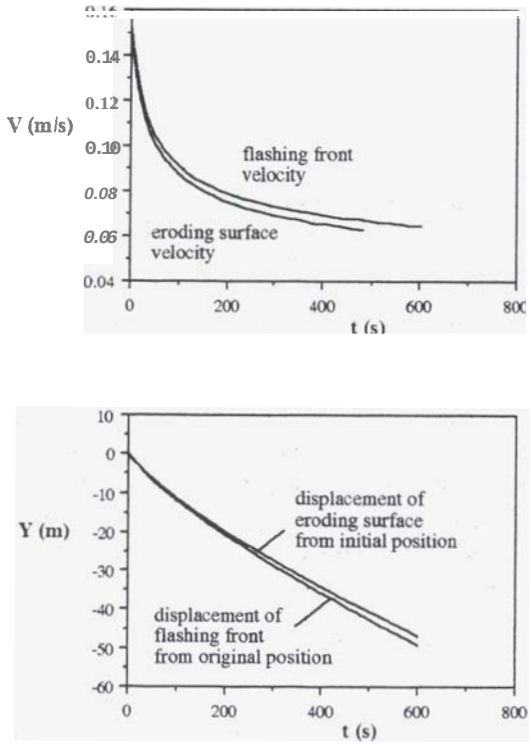

Figure 8 Boundary speeds and displacements for the case k = 10 Darcy, cohesion = 5000 Pa/m over the temperature range T = 110 to 160 'C.

6. GENERAL DISCUSSION

Unfortunately, the work presented on the motion of the boundaries did not reveal anything that would lead to conclusions being drawn on how the eruption is initiated or finally terminated.

It is thought that a triggering event could possibly be a seismic disturbance (Bixley & Browne, 1988). An end to the eruption could be brought about by the redeposition of ejecta back in the vent. This would in effect thicken the flashing zone to the stage where the flashing front comes to a halt. If, as evidence suggests, V is inversely proportional to the thickness, then a thickening process by falling ejecta might act to overcome the mechanism created by an advancing flashing front. The fluid at some point may be below its boiling point at saturated pressure conditions. The flashing front must stop if it reaches a region of rock of negligible porosity. These are just some theories which might explain how the phenomenon eventually ceases.

The only cohesive rock stress considered so far has been that stress in the vertical direction. However, it is known that horizontal stresses exist as a result of rock layer formation stresses which build up over time. The horizontal stress is normally expressed as a proportion of the vertical stress. It is often described in terms of the coefficient of *earth* pressure at rest, K_0, given by

$$K_0 = \frac{\sigma'_{hor}}{\sigma'_{vert}}$$

and σ'_{hor} and σ'_{vert} are the horizontal and vertical effective stresses respectively (Pender, 1990).

In the case of hydrothermal eruptions, at the original surface the soil may be considered as loosely-packed sand or rock breccia in which case K_0 lies in the range 0.4 to 0.5. This implies that horizontal rock stresses may not be important at the beginning of an eruption. As time proceeds the eruption moves down into more densely-packed sand/rock breccia in which case K_0 rises to 1.0 or even 1.5. The horizontal stresses may now dominate and affect the lift condition significantly.

The presence of a crack or vent may allow the flashing fluid to pass with greater ease through the flashing zone to the surface. Small compressive horizontal stresses at the crack surface lead to the crack being opened up by the fluid pressure more readily than if high compressive stresses exist.

Brief exploratory calculations reveal that vertical cohesive stresses in the range 5 to 10 kPa/m were reasonable for our purposes. Denser rock material would require cohesive stresses of 20 to 25 kPa/m to be used.

Future work might include an attempt at linking the underground and above ground flows (McKibbin, 1989) by investigating the similarities between the lift above ground, given by

$$L = \frac{3}{4} C_{ds} \frac{1-\varepsilon}{\varepsilon \phi_s d_p} \rho_f |V_f - V_r| (V_f - V_r)$$

where ε is the voidage, and the pressure gradient below ground is given by the modified Darcy's Law (17). Matching the coefficients of the V_f^2 term in the two equations may be possible. This would represent a major step towards modelling the flow through the air, although two-dimensional effects would also need to be considered.

7. SUMMARY AND CONCLUSIONS

The work described in this paper was fruitful in terms of broadening the understanding of problems associated with modelling hydrothermal eruptions.

The significance of the Forchheimer term in the governing Darcy's Law was addressed. As expected, if form-drag coefficient C was increased, the flashing zone thickness decreased. Properties of interest such as temperature, pressure and lift obeyed already-established trends during the fluid's journey through the flashing zone. Very large pressure gradients were seen to exist near the surface, especially for high values of C. Plots of flashing zone thickness against form-drag coefficient reveal a non-linear relationship. The Forchheimer term only takes on importance for larger rock permeabilities.

The motion of the two moving boundaries, the flashing front and eroding surface, were analysed. It was discovered that the flashing zone thickness increases with time, given that the flashing front propagates along an appropriate temperature gradient. The eroding surface travels more slowly and decelerates faster than the flashing front.

More accurate temperature gradients were calculated on the assumption that the ambient reservoir fluid was a liquid at saturated (boiling) conditions. Brief additional work on cohesive rock stress variations yielded the conclusion that if cohesion is increased, a corresponding decrease in the flashing zone thickness results.

More work on this subject still lies ahead. Attention may now be directed towards modelling the flow more adequately above ground, in the hope that a consistent link in the model between the motion of the fluid below and above ground exists. It is hoped that this work will help further the understanding of the underground process involved with natural hydrothermal eruptions.

NOMENCLATURE

C	form-drag coefficient
C_{ds}	lift coefficient
d_p	diameter of rock particle (m)
ε	voidage
ϕ	porosity
ϕ_s	shape factor
g	acceleration due to gravity (m/s^2)
h	specific enthalpy (J/kg)
k	vertical permeability (m^2, Darcy)
K_0	coefficient of earth pressure
L	dynamiclift (Pa/m)
μ	dynamic viscosity (kg/m s)
m	mass flowrate per unit area (kg/s m^2)
P	pressure (Pa, bar)
q_e	energy flux/unit area (W/m^2)
q_f	Darcy velocity (m/s)
ρ	density (kg/m^3)
Re	Reynolds number
σ'	effective in-situ rock stress (Pa)
S_ℓ	liquid saturation
t	time (s)
T	temperature ("C)
V	flashing front speed (m/s)
v	specificvolume (m3/kg)
V_{er}	eroding surface speed (m/s)
V_f	average particle speed of fluid (m/s)
V_r	average particle speed of rock (m/s)
v_{rat}	volume expansion factor
w_f	fluid volume flowrate per unit area (m/s)
Y	vertical displacement fiom initial surface at atmospheric pressure (m)
z	vertical distance from flashing front (m)

REFERENCES

Bixley, P. F. and Browne, P. R. L. (1988) Hydrothermal eruption potential in geothermal development. Proceedings of the 10th New Zealand Geothermal Workshop 1988, University of Auckland, 195-198.

McKibbin, R. (1989) An attempt at modelling hydrothermal eruptions. Proceedings of the 11th New Zealand Geothermal Workshop 1989, University of Auckland, 1989,267-273.

McKibbin, R. (1990) Mathematical modelling of hydrothermal eruptions. Proceedings of the 1990 International Symposium on Geothermal Energy, Geothermal Resources Council Transactions 14, 1309-1316.

Nield, D. A. (1990) The basic equations for single-phase flow in a porous medium. Unpublished report, Department of Engineering Science, University of Auckland.

Pender, M. J. (1990) Effective stress. Course notes from the paper Special Topic In Engineering Science B, School of Engineering, University of Auckland.